JOURNAL OF MATERIALS SCIENCE: MATERIALS IN MEDICINE 3 (1992) 204–211

# The engineering background of the concept of isoelastic implants

G. HEIMKE, R. J. KOLBE*, R. A. LATOUR Jr
*Department of Bioengineering, College of Engineering, Clemson University, Clemson, SC 29634-0905, USA*

The concept of the so-called isoelastic implant is re-evaluated in three different aspects, using old and basic principles of mechanical engineering. All three are different approaches to the nut and bolt model. The results of these calculations confirm the well-established engineering knowledge that all such essentially cylindrical interfaces necessarily result in a stress concentration in the area beginning (or ending) the load-transmitting interface closest to the point of load application if loaded axially, and that this concentration is more pronounced the more the situation of isoelasticity is approached. Some general conclusions as to the limits of the usefulness of the concept of isoelastic implants and some possible advantages of their applications are outlined in the discussion.

## 1. Introduction

Many modes of failure of bone, joint and tooth replacements have been ascribed to the difference in stiffness of the implants in comparison to the host bone. The shear forces resulting from this mechanical mismatch create relative movements which, in turn, result in the formation of an interfacial pseudoarthrosis seam and subsequent loosening, necessitating the removal of the implant in many cases.

Essentially three alternatives for avoiding the occurrence of interfacial shear movements have been suggested, evaluated experimentally, and studied clinically:

(a) mechanical interlocking,
(b) interfacial bond formation,
(c) adjustment of the stiffness of the implant to that of the surrounding bone.

The introduction of the PMMA bone cement by J. Charnley in 1960 can be regarded as one of the early attempts (and a most successful one) to achieve an interface stability by interlocking [1, 2]. But the formation and reliability of the close bone contact around this cement is compromised not only by its thermal and chemical properties, but also by the unpredictability of the details of the interfacial shape. The absence of thermal and chemical influences with bioinert materials like alumina ceramics [3] allowed for more detailed evaluations of the remodelling processes solely controlled by the stress and strain field created by the insertion of the implant [4]. The subsequent discovery of the "load-line shadow effect" [5] gave further insights about the possibilities and limits for achieving and maintaining a reliable interfacial interlocking along tangentially loaded interfaces [6]. The application of porous coatings to the surfaces of the anchoring portions of bone and joint replacements is another attempt to achieve a reliable fixation of bone substitutes [7].

The discovery of the bone bonding ability of some Ca phosphate-containing glasses and glass–ceramics [8] and of some Ca phosphate ceramics [9] raised much hope for a new and improved mode of implant fixation.

These two kinds of implant fixation have been based on the use of high-modulus metals or ceramics, resulting in an implant stiffness much higher than that of bone. Thus, if a close bone contact could be achieved and was to be maintained, the bond at the bone-to-implant interfaces must be strong enough to withstand all resultant shear forces. All relative movements necessary for load transfer without interfacial shear movements have to be realized by elastic deformations of the surrounding bony tissue.

The basic idea of the third, the isoelastic approach [10], can be regarded as an attempt not to rely completely on the shear-resisting ability of the interface and on the elastic deformability of the surrounding bone. This third alternative must, of course, be combined with either the mechanical interlocking or the bonding approach or their combination (as attempted by coating undulated or porous surfaces with hydroxylapatite), at least along some portions of the interfaces, in order to allow for transmission of the functional loads.

The feasibility of the concept of isoelastic implants has already been evaluated in some previous studies. Calculation of the stress distribution in the simulated bony environment of stems of total hip replacements in an extended, three-dimensional finite-element analysis [11] and the evaluation of these results as a

* Now with Kimberly-Clark, Roswell, GA 30076, USA.



0957–4530 © *1992 Chapman & Hall*

function of the stem stiffness showed a marked increase of the stress concentrations in the calcar region with devices whose stiffness approaches that of the bone. In a finite-element analysis of the stress pattern around dental implants [12] and its dependence on the stiffness of the implant material, the highest stress concentrations were also found if the elastic modulus of the implant approached that of the host tissue. In a more generalized and basic finite-element analysis the stress and strain distribution in two interlocking systems were calculated [13]. The dependence of the interfacial stresses on the stiffness differences also revealed markedly higher stress concentrations for the isoelastic case. This was confirmed *in vivo* by the histological evaluation of implants with mechanical properties closely resembling the situation on which the analysis was based.

These above-mentioned previous discussions all used finite-element calculations. Thus, their results are essentially limited to the particular model chosen in these cases. It is the object of this study to evaluate the concept of isoelastic implants from some well-established basic principles of mechanical engineering [14]. Three different and relatively fundamental approaches will be used; the first is a straightforward treatment, the other two employ closed forward solutions of calculus. This will allow the establishment of rules of general validity on which further conclusions for individual groups of implants can then be based, such as the anchoring of hip and knee replacement, dental, or other load-bearing and transmitting implants.

## 2. Isoelasticity in theoretical mechanics

Most devices, machines and tools in the field of mechanical engineering are made of steel. Thus, all their components consist of materials with nearly identical elastic properties. If they are loaded unidirectionally and their load-bearing cross-sections are similar, they even have similar stiffnesses.

### 2.1. The nut and bolt model

The nut and bolt combination can be regarded as one of the most widely used means of fixation. In the schematic cross-sectional representation of Fig. 1, the nut and bolt are interlocked by the three threads $T_1$–$T_3$ with the axial distance $l_1$ between consecutive threads. The load-bearing cross-sectional areas ($A$) of the nut (index N) and bolt (index B) are assumed to be $A_N$ and $A_B$ and their elastic moduli $E_N$ and $E_B$, respectively. The forces $F_B$ are applied to the bolt while the nut is supported by the forces $F_N$. If there is any portion d$F$ of the forces $F_B$ transmitted to the nut via the first thread $T_1$, the remaining force $F - \mathrm{d}F$ will have to be transmitted by one of the other threads. The segment $l_1$ of the bolt between the first and the second thread will be under tension and, thus, be elongated by an amount

$$\mathrm{d}l_{B1} = \frac{F - \mathrm{d}F}{E_B A_B} l_1$$

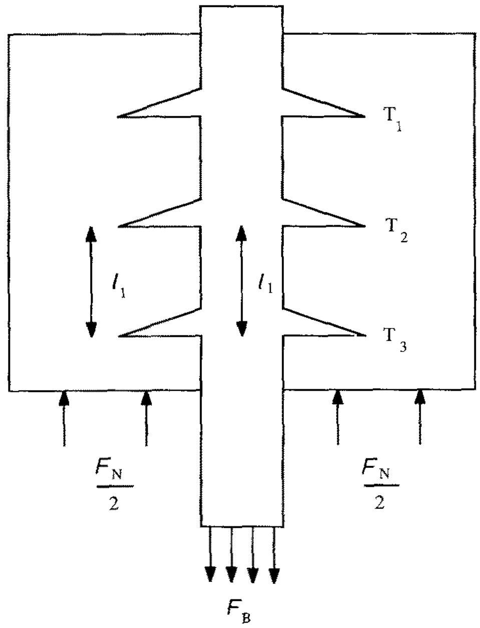


*Figure 1* Nut and bolt model with homogeneously distributed forces acting on the bolt $F_B$ and supporting the nut $F_N$ ($F_B = F_N$), the threads T and the interthread length $l_1$.

This same remaining force will have to be transmitted through the segment $l_1$ of the nut as a pressure (normal stress) causing a length reduction of

$$\mathrm{d}l_{N1} = \frac{F - \mathrm{d}F}{E_N A_N} l_1$$

Thus, if secondary effects like deformations of the steps themselves are disregarded, all forces will be concentrated completely on the first thread, because, otherwise, the next thread would lose contact.

Somewhat more quantitatively, the total displacement along the interface between the first and the second threads will be (with $1/E_B A_B = 1/S_B$ and $1/E_N A_N = 1/S_N$ as stiffness coefficients, $\mathrm{d}S = S_B - S_N$, and replacing $S_B$ by $S_N + \mathrm{d}S$)

$$\mathrm{d}l_1 = (F - dF)l_1 \frac{\mathrm{d}S + S_N + S_N}{S_N(S_N + \mathrm{d}S)}$$

$$= (F - \mathrm{d}F)l_1 \frac{2S_N + \mathrm{d}S}{S_N^2 + S_N \mathrm{d}S}$$

For $\mathrm{d}S = 0$, the case of identical stiffnesses of bolt and nut, this results in an interfacial displacement

$$\mathrm{d}l_1 = (F - \mathrm{d}F)l_1 \frac{2}{S_N}$$

and for $\mathrm{d}S = S_N$ and $\mathrm{d}S = 9S_N$, equivalent to $S_B = 2S_N$ and $S_B = 10S_N$,

$$\mathrm{d}l_1 = (F - \mathrm{d}F)l_1 \frac{3}{2S_N}$$

and

$$\mathrm{d}l_1 = (F - \mathrm{d}F)l_1 \frac{11}{10S_N}$$

Thus, the larger the stiffness of the bolt the smaller the interfacial displacement and, thus, the interfacial shear

TABLE I The (normalized) interfacial displacement $dl_1$ (as an indication of the interfacial shear stresses) as a function of the stiffness differences $dS$ between the nut and the bolt

| $dS = S_B - S_N$ | $dS = 0, S_B = S_N$ (isoel. case) | $dS = S_N, S_B = 2S_N$ | $dS = 9S_N, S_B = 10S_N$ (CoCrMo on bone) |
|---|---|---|---|
| $dl_1 S_N / l_1(F - dF)$ | 2 | 1.5 | 1.1 |

stresses, as can clearly be realized from the summary given in Table I. The stiffness ratio of 1:10 is about equivalent to the stiffness ratio between cortical bone and the Co-based alloys. In a similar manner it can be shown that, in the case of a tensional force acting on the nut on its opposite surface, the loads will be concentrated on the two most outside threads only.

## 2.2. The nut and shaft model

The nut and bolt model can be refined by increasing the number of threads and simultaneously decreasing their thicknesses and distances until the situation of a homogeneously bonded system is reached (Fig. 2) [15]. This model can be used to quantitatively derive the shearing forces along the nut and shaft interface. The outside boundaries are assumed to be rigidly fixed.

The forces $F_y$ acting on any segment of the shaft with the width $d'y$ ($d'$ indicating a "difference") in static equilibrium can be described (Fig. 2) as

$$\sum F_y = 0: \quad P(y) - P(y + d'y) - \tau A = 0 \tag{1}$$

where the deformations resulting from the outside force are

$$P(y) = \sigma_y \pi a^2 = E_S \varepsilon_y \pi a^2 = E_S \frac{d'u}{d'y} \pi a^2$$

$$\varepsilon_y = \frac{d'u}{d'y}$$

with the normal stress and strain $\sigma_y$ and $\varepsilon_y$, respectively, in the $y$ direction and the shear strain along the cylindrical shaft to nut interface being

$$\tau = G_N \frac{u(y) - u(w)}{l} = G_N \frac{u(y)}{l}$$

and the interfacial area

$$A = 2\pi a d'y$$

(It should be noted that $E_S$ and $G_N$ refer to the elastic modulus of the shaft and shear modulus of the nut, respectively). Substituting the area $A$ into Equation 1 and dividing through by $d'y$ yields

$$\frac{P(y) - P(y + d'y)}{d'y} - 2\pi\tau a = 0$$

which, in changing from differences to differentials (from $d'$ to $d$), can be written as

$$\frac{dP}{dy} - 2\pi\tau a = 0 \tag{2}$$

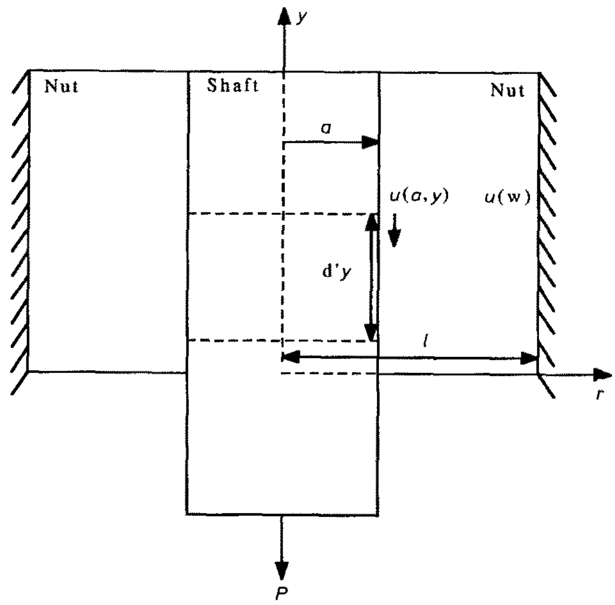


*Figure 2* Nut and shaft model with characteristic variables used in the text: $P$ = pulling force, $a$ = radius at nut–shaft interface, $l$ = outer radius of nut ($l - a$ = constant), $u(\mathrm{w})$ = point at wall, $u(a, y)$ = displacement in $y$ direction at nut–shaft interface, $d'y$ = (differential) shaft segment in $y$ direction.

and, using the definitions following Equation 1,

$$\frac{d}{dy}\left(E_S \pi a^2 \frac{du}{dy}\right) - \frac{G_N}{l} 2\pi a u(y) = 0$$

which can be reduced to

$$\frac{d^2u}{dy^2} - \frac{2G_N}{E_S a l} u(y) = 0 \tag{3}$$

Equation 3 is a second-order linear differential equation with real constant coefficients. Its solution (for the boundary condition as $y \to \infty$, $p \to 0$, and with $E_N$ and $\nu_N$ refering to the elastic modulus and Poisson's ratio of the nut, respectively) yields for the interfacial shear stress

$$\tau = -\frac{P}{\pi a}\left(\frac{G_N}{2aE_S l}\right)^{1/2} \exp\left[-\left(\frac{E_N}{E_S a l(1 + \nu_N)}\right)^{1/2} y\right]$$

or, using the correlation between the shear and elastic moduli $G_N = E_N/[2(1 + \nu_N)]$,

$$\tau = -\frac{P}{2\pi a}\left(\frac{E_N}{E_S(1 + \nu_N) a l}\right)^{1/2} \times \exp\left[-\left(\frac{E_N}{E_S a l(1 + \nu_N)}\right)^{1/2} y\right]$$

With the introduction of the ratio of the two elasticities as $E_N/E_S = R$ and summarizing all other terms in constants, this equation can be used to express the dependence of the shear forces on the variation of the differences of the elastic moduli for any given interfacial position $y$:

$$\tau = -c'R^{1/2}\exp - [(c''R)^{1/2}y] \qquad (4)$$

Keeping $E_N$ = constant and, thus, also $\nu_N$ = constant, and letting $E_S$ increase from 1 (the isoelastic case) to 10 (the elasticity ratio of Co-based alloys to cortical bone), the dependence of the interfacial stress can be plotted as a function of the ratio $R = E_N/E_S$ as shown in Fig. 3 ($E_N = 1$, $c' = c'' = 1$, $y = 1$).

Thus, the highest interfacial stresses do occur in the isoelastic situation. The dependence of the stresses on the length of the bolt ($y$) yields a stress concentration at the entrance of the bolt into the nut (at $y = 0$) and an exponential decrease for deeper penetrations (increasing $y$).

## 2.3. The punching model

Another approach to the description of the interfacial stresses in a truely isoelastic case can be derived from the theory of punching.

If a punch is resting on a half-space as indicated schematically in Fig. 4, the cylinder underneath the punch with radius $a$ (which is to be punched out) will, of course, be isoelastic with regard to the surrounding material and, in addition, will be bonded to it homogeneously. As far as implants are concerned, this type of bonding will be the most ideal case, as hoped may be obtainable with bioactive materials like hydroxylapatite ceramics [16].

To derive the stress components along the surface of the cylinder, first, a single, infinitely long, line-shaped load acting on a half-space is considered as shown in Fig. 5 [17]. With this load per unit line length $p$, it can be shown that [17]

$$\sigma_\theta = \tau_{r\theta} = 0$$

Also, with the sum of all forces in the $y$-direction being equal to zero (principle of static equilibrium), it follows that

$$\sum F_y = 0: \quad -P + \int_{-\pi/2}^{\pi/2} \sigma_r \cos\theta \, r d\theta = 0$$

and with $\sigma_r = C\cos\theta/r$ ($C$ = some constant)

$$P = \int_{-\pi/2}^{\pi/2} C\cos^2\theta \, d\theta$$

yielding $C = 2P/\pi$, resulting an $\sigma_r = (-2P/\pi r)\cos\theta$.

For a plane at a distance $y$ parallel to the surface of the half-space, the normal and shear components of the stress at a point C (Fig. 6) T and M can be found using the equations in accordance with Mohr's circle

$$\sigma_x = \frac{\sigma_r + \sigma_\theta}{2} + \frac{\sigma_r - \sigma_\theta}{2}\cos 2\theta + \tau_{r\theta}\sin 2\theta$$

$$\sigma_y = \frac{\sigma_r + \sigma_\theta}{2} - \frac{\sigma_r - \sigma_\theta}{2}\cos 2\theta + \tau_{r\theta}\sin 2\theta$$

$$\tau_{xy} = \frac{\sigma_r - \sigma_\theta}{2}\sin 2\theta + \tau_{r\theta}\cos 2\theta$$

This gives for the stresses indicated in Fig. 7

$$\sigma_x = \frac{-2P\cos^4\theta}{\pi y}$$

$$\sigma_y = \frac{-2P\sin^2\theta\cos^2\theta}{\pi y}$$

$$\tau_{xy} = \frac{-2P\sin\theta\cos^3\theta}{\pi y}$$

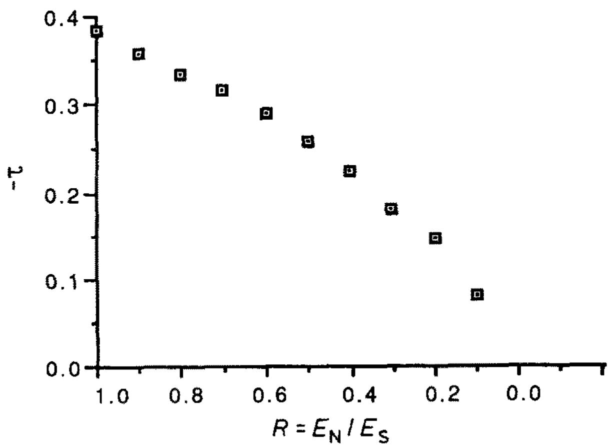


*Figure 3* Interfacial shear as a function of the ratio of the elastic moduli following from the nut and shaft model according to Equation 4 with $c' = c'' = y = 1$.

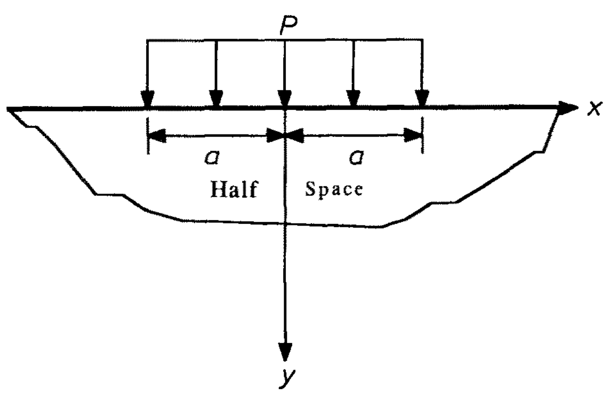


*Figure 4* Punch $P$ on half-space.

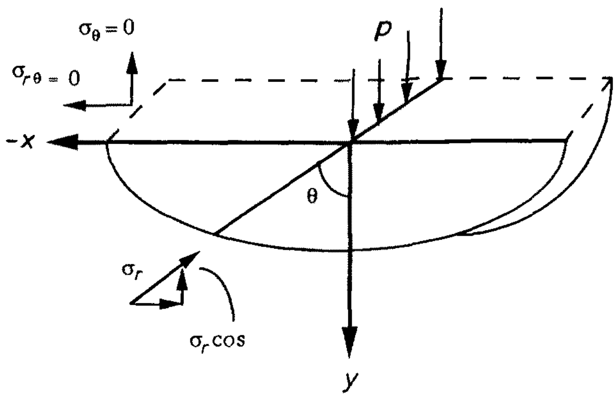


*Figure 5* Single linear load on a half-space with indication of radial component of stress.

If the load $P$ is applied at a distance $\Omega$ away from the origin (Fig. 8), this must be rewritten

$$\begin{aligned}\sigma_x &= \frac{-2Py^3}{\pi r^4}\\ \sigma_y &= \frac{-2P(x+\Omega)^2 y}{\pi r^4} \qquad (5)\\ \tau_{xy} &= 2P(x+\Omega)y^2\end{aligned}$$

If these loads $P$ are applied continuously between the limits

$$x = -a \leqslant \Omega \leqslant x = +a$$

the resulting stresses in the infinite half-space subject to the combined action of these loads can be found by integration of Equations 5 between these limits (with $P_0$ being the total load within these limits), using standard mathematical tables:

$$\begin{aligned}\sigma_x &= \frac{-P_0}{\pi}\left[\tan^{-1}\left(\frac{x+a}{y}\right) - \frac{(x+a)y}{(x+a)^2+y^2} - \tan^{-1}\left(\frac{x-a}{y}\right) + \frac{(x-a)y}{(x-a)^2+y^2}\right]\\ \sigma_y &= -\frac{P_0}{\pi}\left[\tan^{-1}\left(\frac{x+a}{y}\right) + \frac{(x+a)y}{(x+a)^2+y^2} - \tan^{-1}\left(\frac{x-a}{y}\right) - \frac{(x-a)y}{(x-a)^2+y^2}\right] \qquad (6)\\ \tau_{xy} &= -\frac{P_0}{\pi}\left[\frac{y^2}{(x-a)^2+y^2} - \frac{y^2}{(x+a)^2+y^2}\right]\end{aligned}$$

These stress components were calculated with the values $P = 1$, $a = 1$, $x$ varying from 0 to 10 in increments of 0.1, and $y = 0.1, 0.5, 0.9, 0.991, 1.001, 1.1, 1.5, 1.9$ and are presented graphically in Figs 9, 10 and 11. Each graph contains 13 plotted points corresponding to the depth values $y = 0$, $y = 0.1$, and $y = 1$ to 10 in integer steps. Note that $x = 1$ represents the (hypothetical) walls of the cylinder underneath the edges of the punch (because of the tangent function, there is a discontinuity at $y = 0$ and $x = a$).

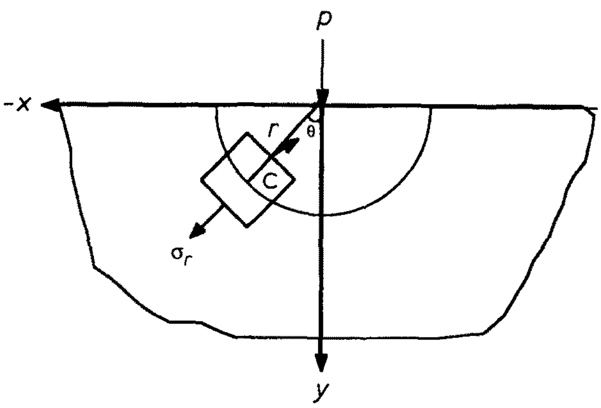


*Figure 6* As Fig. 5 to demonstrate internal equilibrium of forces acting on the volume element C.

## 3. Discussion

All three evaluations of the problem of interfacial stresses at the junction of two components use different approaches. All of them do show a marked concentration of the stresses at the entrance of this device into its encagement. The first two evaluations, the bolt and nut as well as the shaft and nut models, express this stress concentration as a function of the ratio of the elastic moduli of the materials concerned. Their results show that this concentration becomes more pronounced as the state of isoelasticity is approached.

Thus, it must be generally concluded for stem or post-shaped load-bearing and transmitting implants that

(i) the shear forces between the implant and the surrounding bony tissue will always be the highest at the interfacial area closest to the zone of load application, and

(ii) the degree of this interfacial stress concentration increases as the state of isoelasticity (or, rather, equality of stiffness) is approached.

The concept of isoelastic implants had mostly been suggested for the anchorage of total hip replacements [10. 18]. But, of course, there is no reason not to consider this concept for other hard-tissue replacements, as had been done for dental implants [12]. In

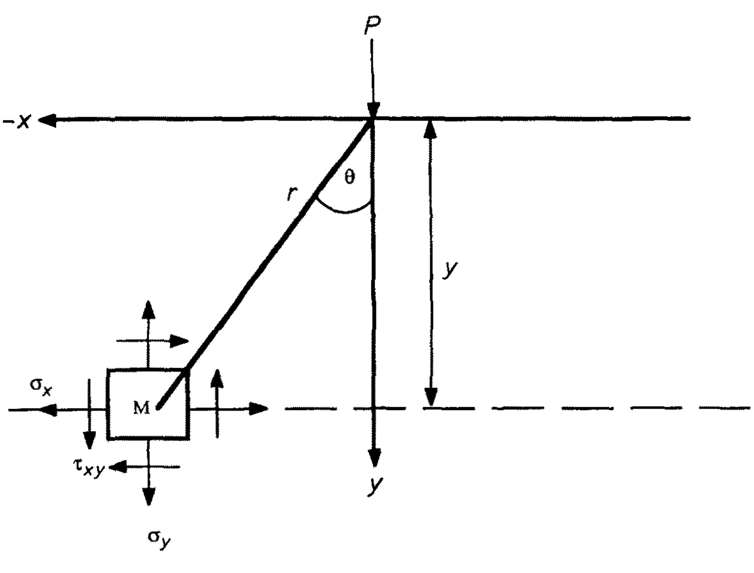


*Figure 7* As Figs 5 and 6 to demonstrate the normal and shearing components acting on a volume element M in rectangular coordinates at a distance $y$ from the surface of the half-space.

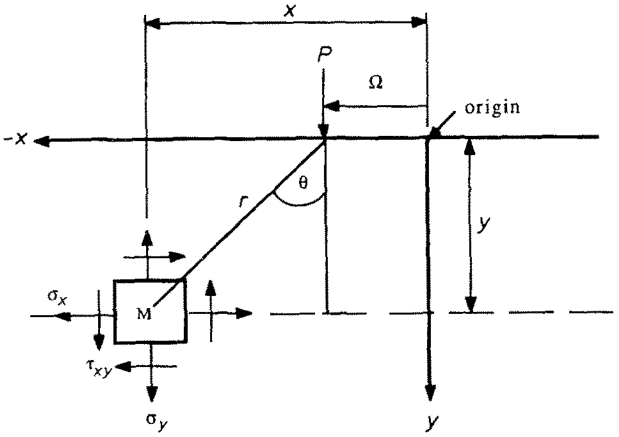


*Figure 8* Load $P$ on half-space as in Fig. 7 but shifted from the origin in the $-x$ direction by the amount $\Omega$: $y = r\cos\theta$, $x = \Omega + r\sin\theta$, $r = [y^2 + (x+\Omega)^2]^{1/2}$.

all these considerations the conclusions mentioned above must be kept in mind. If the interfacial stress concentrations cause pressure necrosis or surpass the fatigue limit of the implant material locally, a stiffer implant must be chosen. However, an isoelastic implant can be used and may even be the solution of choice if a high stress concentration appears to be desirable at that location, provided the stresses do not surpass the above limits.

In total hip surgery, some concentration of load transfer from (collarless) stems into the femur in the area of the calcar femoris is desirable from the point of view of avoiding disuse atrophy in the proximal femur. Thus, if the limits mentioned above are not surpassed, isoelastic stems can be considered.

The stress concentrations resulting from the calculations presented here and those given elsewhere [11–13] seem to contradict the conclusions of strain-gauge measurements of loaded models or cadaver femurs carrying implants of different stiffnesses (e.g. [18]). They report on deformations of the outside contour of the femur which more closely approach the natural situation for isoelastic than for stiffer stems. If a bond was provided at all in these measurements as assumed to exist in our calculations, the solution of this apparent discrepancy may be provided by the considerations of the previous paragraph. The concentration of the load transfer to the calcar area is very close to the natural case, and the bending behaviour of the more distal portions of the isoelastic stem will alter the deformation behaviour of the femur less than a stiffer stem.

In dentistry, isoelastic implants have been taken into consideration in order to account for the relatively large deformations of the mandible and the still larger deformations in the maxilla [19] during swallowing and biting. The stiffer and more extended the implants are, the larger the forces which must be supported by the interfacial bond between the implants and the adjacent bony tissue. These interfacial stresses are hoped to be minimized if the implant can deform in a manner similar to the surrounding bone.

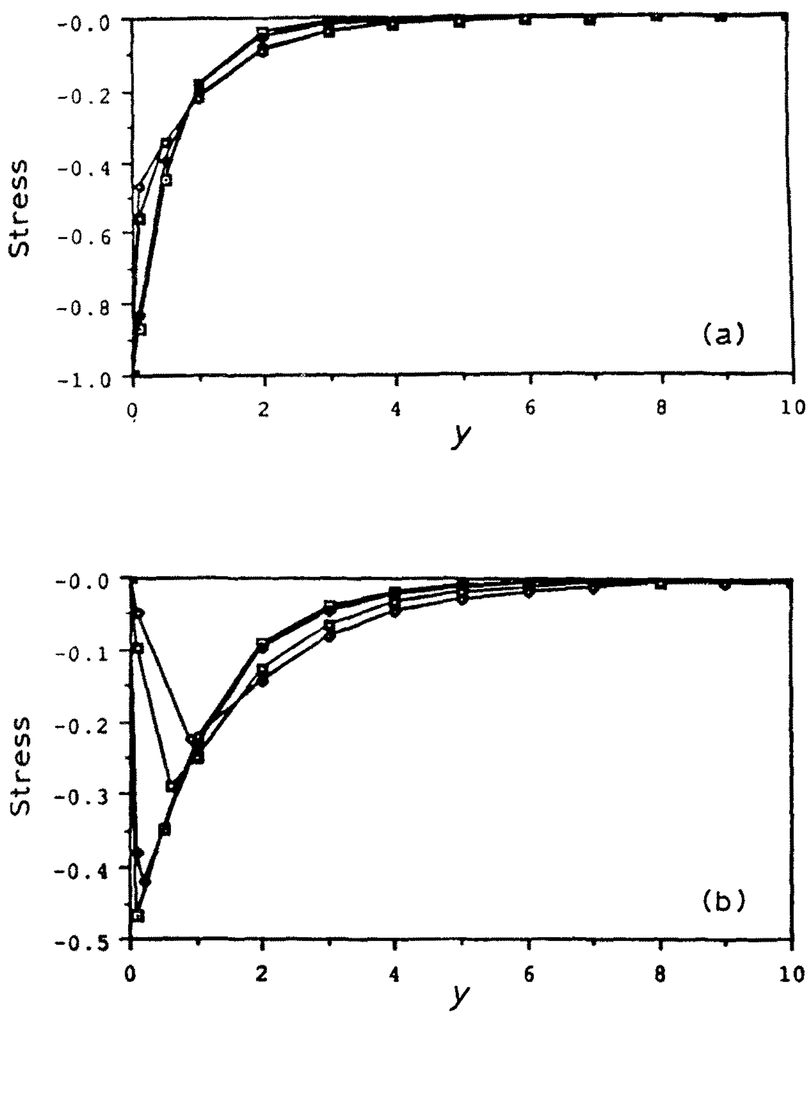


*Figure 9* Normal stresses in the horizontal $x$ direction as a function of depth ($y$ direction) for different cylindrical surfaces ($x$) according to Equation 6. (a) $x$ = (□) 0.1, (◆) 0.5, (□) 0.9, (◇) 0.991; (b) $x$ = (□) 1.001, (◆) 1.1, (□) 1.5, (◇) 1.9.

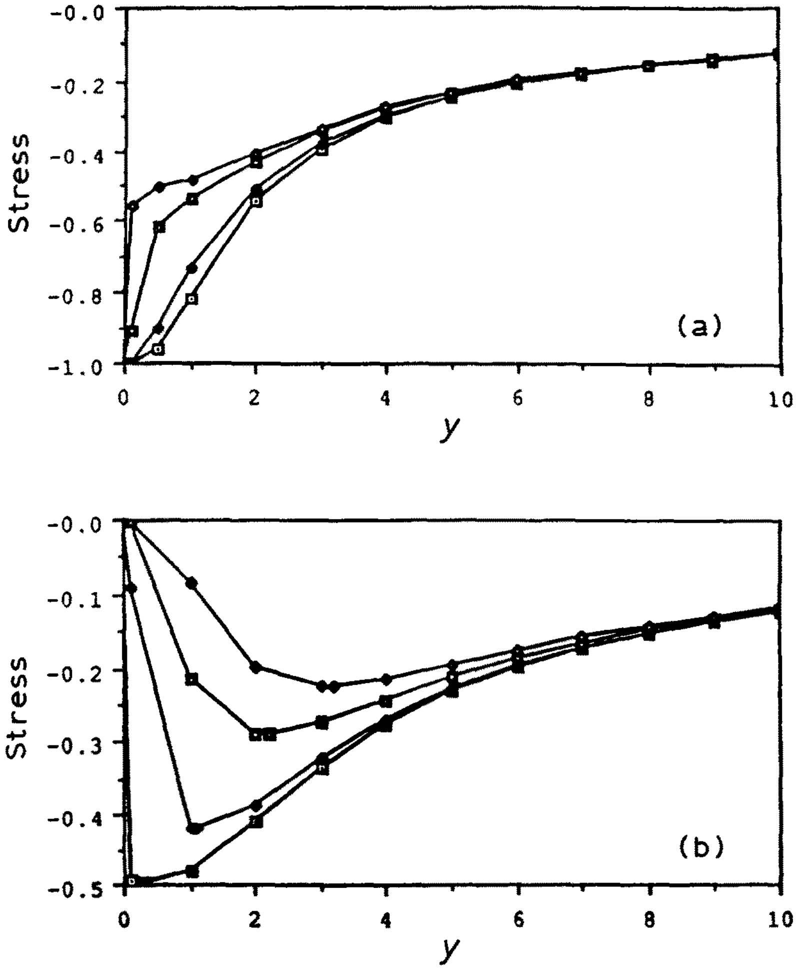


*Figure 10* Normal stresses in the $y$ direction as a function of depth ($y$ direction) for different cylindrical surfaces ($x$) according to Equation 6. (a) $x =$ (⊡) 0.1, (◆) 0.5, (□) 0.9, (◇) 0.991; (b) $x =$ (⊡) 1.001, (◆) 1.1, (□) 1.5, (◇) 1.9.

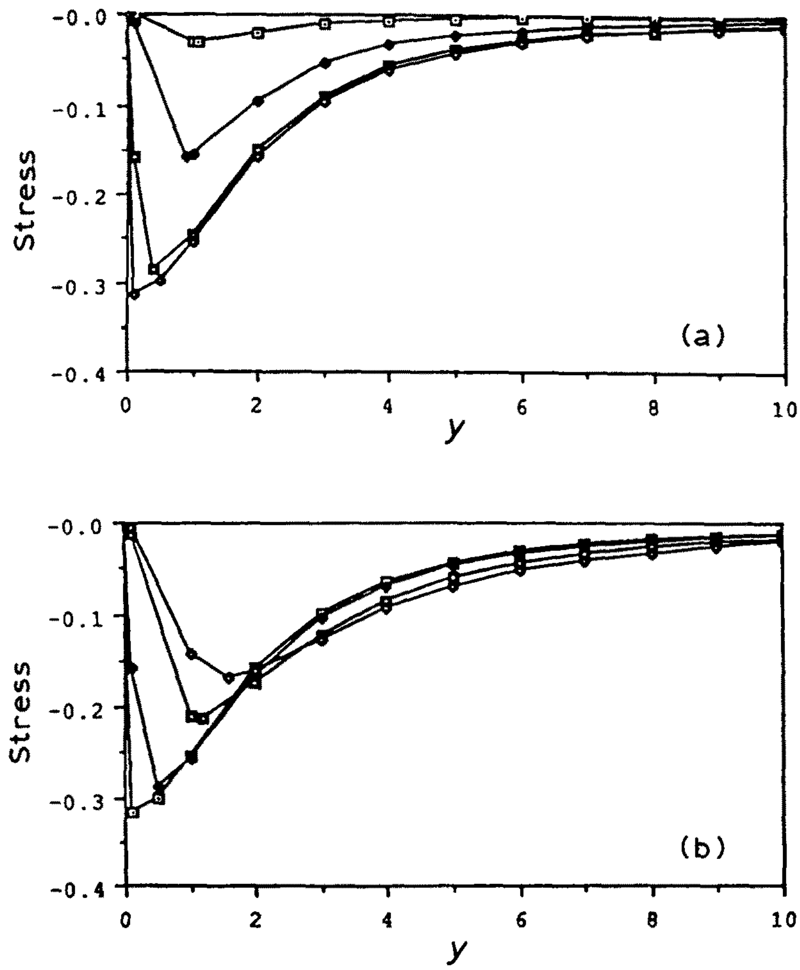


*Figure 11* Shear stresses for different cylindrical surfaces ($x$) as a function of depth ($y$ direction) according to Equation 6. (a) $x =$ (⊡) 0.1, (◆) 0.5, (□) 0.9, (◇) 0.991; (b) $x =$ (⊡) 1.001, (◆) 1.1, (□) 1.5, (◇) 1.9.

The results of the calculations presented above do not exclude this possibility. On the contrary, their due consideration rather allows the best compromise between the desired deformability and the necessity to avoid stress concentrations to be found.


## Acknowledgements

The authors thank Professors J. G. Goree and I. Haque, Clemson, SC for their advice and assistance.


## References


1. J. CHARNLEY, *Br. J. Bone Joint Surg.* **46** (1964) 518.
2. *Idem.*, "Acrylic Cement in Orthopaedic Surgery" (Williams and Wilkins Co., Baltimore, 1972).
3. S. F. HULBERT, F. A. YOUNG, R. S. MATHEWS, J. J. KLAWITTER, C. D. TALBERT and F. H. STELLING, *J. Biomed. Mater. Res.* **4** (1970) 433.
4. P. GRISS, R. SILBER, B. MERKLE, G. HEIMKE and B. KREMPIEN, *J. Biomed. Mater. Res. Symp.* **7** (1976) 519.
5. C. M. BÜSING, G. HEIMKE, W. SCHULTE and W. LINN, *Pathologe* **1** (1979) 61.
6. G. HEIMKE, W. SCHULTE, B. d'HOEDT, P. GRISS, C. M. BÜSING and D. STOCK, *Int. J. Artif. Org.* **5** (1982) 207.
7. H. HAHN and W. PATICH, *J. Biomed. Mater. Res.* **4** (1970) 571.
8. L. L. HENCH, R. J. SPLINTER, W. C. ALLEN and T. K. GREENLEE, *J. Biomed. Mater. Res. Symp.* **2** (1971) 117.
9. S. R. LEVITT, P. H. CRAYTON, A. A. MONROE and R. A. CONDRATE, *J. Biomed. Mater. Res.* **3** (1969) 3.
10. E. MORSCHER, R. MATHYS and H. R. HENCH, in "Advances in Hip and Knee Joint Technology–Engineering in Medicine", Vol. 2, edited by M. Schaldach and D. Hohmann (Springer, Berlin, 1976) p. 402.
11. R. SCHOLTEN and H. RÖHRLE, in "Trends in Biomechanical Engineering", edited by S. K. Gupta (CBME Publications, New Delhi, 1978) p. 148.
12. U. SOLTESZ and D. SIEGELE, *Dtsch. Zahräztl. Z.* **39** (1984) 183.
13. R. HUISKES, in "Biomechanics 1983", edited by P. Ducheyne, G. Van der Perre and A. E. Aubert (Elsevier, Amsterdam, 1984) p. 37.
14. G. HEIMKE, in "Osseo-Integrated Implants", Vol. I, "Basics, Materials, and Joint Replacements", edited by G. Heimke (CRC Press, Boca Raton, 1990) p. 1.
15. B. KENNY and E. A. PATTERSON, *J. Strain Anal.* **20**(1) (1985) 35.
16. G. de LANGE, C. de PUTTER and K. de GROOT, in "Osseo-Integrated Implants", Vol. II, "Implants in Oral and ENT Surgery", edited by G. Heimke (CRC Press, Boca Raton, 1990) p. 209.
17. S. P. TIMOSHENKO and J. N. GOODIER, "Theory of Elasticity", 3rd Edn. (McGraw-Hill, New York, 1970).
18. R. D. AINSWORTH, R. R. TARR and L. CLAES, in Proceedings of 1st International Conference on Composites in Bio-Medical Engineering, London, November 1985, pp. 23/1–23/7.
19. W. SCHULTE, Tübingen Private Communication (1989).



*Received 1 October 1990*
*and accepted 6 February 1991*